European Polymer Journal 204 (2024) 112714

Contents lists available at ScienceDirect

European Polymer Journal

journal homepage: www.elsevier.com/locate/europolj

Tuning Pluronic F127 phase transitions by adding physiological amounts of salts: A rheology, SAXS, and NMR investigation

Giovanni Russo [a], G. Rossella Delpiano [a], Cristina Carucci [a,b], Massimiliano Grosso [b,c], Claudia Dessì [c], Olle Söderman [d], Björn Lindman [d,e], Maura Monduzzi [a,b,*], Andrea Salis [a,b,*]

[a] Dipartimento di Scienze Chimiche e Geologiche, University of Cagliari, SS 554, Bivio Sestu, 09042 Monserrato, CA, Italy
[b] Consorzio Interuniversitario per lo Sviluppo dei Sistemi a Grande Interfase (CSGI), via della Lastruccia 3, 50019 Sesto Fiorentino, FI, Italy
[c] Dipartimento di Ingegneria Meccanica Chimica e dei Materiali, University of Cagliari, Via Marengo, 2, 09123 Cagliari, Italy
[d] Division of Physical Chemistry, University of Lund, P.O. Box 124, S-221 00 Lund, Sweden
[e] Coimbra Chemistry Centre, Department of Chemistry, University of Coimbra, Rua Larga, 3004-535, Coimbra, Portugal

ARTICLE INFO

Keywords:
Pluronic F127
Hofmeister series
Thermoresponsive hydrogels
Tunable phase transitions

ABSTRACT

Specific ion (Hofmeister) effects in colloid and biological systems represented a scientific challenge for more than 100 years. Recently, possible applications, based on their rationalization, are emerging. Here, Cl^-, SO_4^{2-}, SCN^- anions and Na^+, K^+, Mg^{2+} cations are added at physiological concentration (~0.15 mol/kg) to Pluronic F127 20 wt% aqueous solutions to suitably tune phase transitions for a smart drug delivery platform. Rheological measurements, along with SAXS and NMR self-diffusion experiments, are used to carefully characterize the prepared F127/salt-based formulations. The critical micellar temperature (cmt), the hard-gel formation temperature (T_{hg}), liquid crystal structures, and self-diffusion coefficients are determined. The cmt and T_{hg} values of F127/salt formulations are lower than that of F127 20 wt% sample, following an anionic Hofmeister series: $SO_4^{2-} < Cl^- < SCN^-$. All added salts significantly increase storage modulus and complex viscosity with maximum values occurring at T around 40 °C. SAXS data confirm that added salts preserve cubic liquid crystal phases. NMR self-diffusion analysis highlights that the intermolecular interactions and mobility of F127 unimers/aggregates are ion specific at 16 °C but not at 40 °C. These findings suggest that F127/salt-based formulations may constitute a versatile thermosensitive platform for drug delivery able to assure sustained release in topical or surgery administrations, in the range of temperatures 30–45 °C.

1. Introduction

Stimuli-responsive polymers respond to small variations in environmental conditions, like pH, temperature, etc., leading to a sharp change in their properties. This peculiar behavior allows, with a careful study of the physico-chemical characteristics of the polymer, their use as drug delivery systems with the ability to administer controlled and self-regulated drugs [1–6]. Among many interesting polymers those which form thermosensitive hydrogels, based upon nonionic copolymers such as the Pluronic family, have attracted much attention because of their huge versatility in terms of composition, transition temperature, type of drugs that can be entrapped, as well as type of administration route, spanning from injectable fluids to topical formulations or tissue engineering [7–13]. Moreover, other stimuli responsiveness can be introduced through suitable functionalization of the copolymer or adding other components (biomacromolecules, polyelectrolytes, etc) [14–18].

Pluronic® F127 (F127) is a non-ionic hydrophilic three-block copolymer, ABA structure, composed of a central hydrophobic block of polypropylene oxide (PO) and two external hydrophilic blocks of polyethylene oxide (EO), having an approximate formula $EO_{97}PO_{68}EO_{97}$ and a MW ≈ 12.5 kDa. Previous works have investigated the phase behavior of F127 with focus on the critical temperatures related to micelle formation (cmt), sol–gel transition, cubic liquid crystal (LC) formation, and cloud point [3,4,18–25]. Gelation is often found to occur through two steps, namely a first sol–gel (hard gel) transition, then, by further increasing the temperature, a hard-soft gel transition just before the cloud point. The hard gel was characterized as a cubic LC phase having simple cubic (SC) [26], face centered (fcc) [20,21] or body centered (bcc) [19,27] cubic lattice, depending on temperature, composition, purity of the copolymer as well as the presence of

* Corresponding authors at: Dipartimento di Scienze Chimiche e Geologiche, University of Cagliari, SS 554, Bivio Sestu, 09042 Monserrato, CA, Italy.
E-mail addresses: monduzzi@unica.it (M. Monduzzi), andrea.salis@unica.it (A. Salis).

https://doi.org/10.1016/j.eurpolymj.2023.112714
Received 4 November 2023; Received in revised form 18 December 2023; Accepted 22 December 2023
Available online 25 December 2023

additives. The hard-soft gel transition has been related to a less favorable interaction between the aqueous solvent and the EO chains at higher temperature, in turn reflecting a decreased polarity of the polymer. As discussed further below this results in a decrease in volume of the polymer micelles and, therefore, a weakened repulsion between them [1,3,26]. We should notice that often, however, the hard-soft gel transition and clouding (as discussed below) cannot be clearly distinguished [18,23]. The temperatures involved in the different transitions are highly dependent of F127 concentration. In the absence of other components, the phenomenon of gelation is generally reversible. In addition, the lowest critical solution temperature (LCST) depends on concentration and generally ranges between 25 and 37 °C, in the absence of any additives [14,28,29]. No gelation was recorded for copolymer concentrations lower than about 17 wt% in the range of temperature up to 60–70 °C [17,19,30]. The phase behavior and the critical temperatures of F127 can significantly be modified by the addition of drugs, excipients and other compounds [31–34]. Depending on the needed performance of the formulation, particularly the type of administration, a tuning of the transition temperatures can be attained through a careful choice of added electrolytes in suitable concentration.

The effects associated with the addition of electrolytes on the behavior of macromolecules has widely been investigated since the pioneering work by F. Hofmeister in 1888 [35,36]. He found that the egg white proteins solubility in water (salting in) in the presence of anions increases in the order: $SO_4^{2-} < F^- < Cl^- < Br^- < NO_3^- < I^- < ClO_4^- < SCN^-$, and for cations in the order $Cs^+ < NH_4^+ < Rb^+ < K^+ < Na^+ < Li^+ < Ca^{2+} < Mg^{2+}$ the effect of cations being generally less evident than that of anions [37]. Different explanations of this universal sequence have been proposed. Ions have been classified as kosmotropic (order makers) and chaotropic (disorder makers) depending on their effects on water structure [38–41]. More recently, the contribution of dispersion forces due to ion polarizability has been considered [42,43]. In the presence of proteins or polar polymers, ions may promote intricate phenomena involving hydration of both ions and chains, and ion-macromolecule interactions [44–50].

The aim of the work is to obtain a drug delivery platform based on the thermosensitive Pluronic F127 where the transition temperatures can easily be tuned adding physiological concentration (0.05–0.15 mol/kg) of salts, depending on the type of administration route. Remarkably, Pluronic F127 is one of the few copolymers of the Pluronic family that are involved in clinical trials:[51] this fact provided a further motivation to revisit F127 phase behavior in the presence of substances that can tune phase transition temperatures. To do that, we investigate in detail the transition temperatures of F127 (20 wt%), particularly the range of stability of the LC gel in the presence of salts, using rheology, small angle X-ray scattering (SAXS) and NMR techniques. We will show that temperature ramps, at constant oscillation frequency, can provide detailed information on the changes in cmt, and sol–gel transition temperatures. To clarify the effects of salts on Pluronic F127 self-assembly and phase behavior, SAXS experiments were performed at 40 °C to ascertain the occurrence of cubic LC gel phases [19,26,27]. Finally, additional information related to the molecular motions was obtained from NMR self-diffusion experiments at different temperatures.[18,25].

2. Experimental

2.1. Chemicals and sample preparation

Pluronic® F127 (approximate formula $EO_{97}PO_{68}EO_{97}$, $M_W \approx 12.5$ kDa), NaCl (99.0 %), $MgCl_2$ (98.0 %), NaSCN (99.0 %) and D_2O (99.9 %), were purchased from Sigma Aldrich. KCl (>99.5 %) and Na_2SO_4 (>99.0 %) were from MERCK-Schuchardt. All reagents were used as received.

A stock solution of F127 (20 wt%) was prepared in MilliQ water containing 20 wt% of D_2O. Then, samples containing salts were prepared by weighing the appropriate quantities of stock solution and salt to obtain about 10 mL of each sample. All samples, including the stock solution, were equilibrated at 4 °C, under gentle shaking, for 24 h. Each sample was prepared in triplicate and stored at 4 °C. No phase separation, or salt crystallization was observed during storage for at least 6 months.

2.2. Rheological measurements

A stress/strain controlled rheometer MCR 102 (Anton Paar, Graz, Austria) equipped with a plate-plate geometry (plate diameter = 50 mm, gap width = 0.5 mm) was used to carry out rheological measurements. A Peltier system (accuracy of ± 0.1 °C) was used to control the temperature of the bottom plate. Rheological data were collected through the software RheoCompass™ (Anton Paar, Graz, Austria). The samples were loaded on the bottom plate from a glass tube stored at 4 °C. Silicon oil was used to seal the cover plate after sample deposition. Dynamic temperature ramp experiments (Heating rates of 1 °C min^{-1}) were performed in the range of temperatures from 10 to 85 °C, whereas for samples containing 0.15 mol/kg Na_2SO_4 or 1 mol/kg NaCl heating ramps started from 0 °C. The cooling ramp needed to ascertain the reversibility of the phase transitions observed during heating was performed using a cooling rate of 0.2 °C/min. The linear viscoelastic regime (LVER) was ascertained using amplitude sweep experiments at $\omega = 1$ Hz and a shear strain of 1.0 %.

G' (storage modulus) and the G" (loss modulus), the elastic and viscous component, respectively, are defined in Eq. (1) in terms of the maximum amplitude of the stress (γ_0), the maximum amplitude of the strain (γ_0), $\omega = 2\pi f$ (f = frequency), and the loss angle (δ).

$$G' = \frac{\sigma_0}{\gamma_0}\cos\delta, G'' = \frac{\sigma_0}{\gamma_0}\sin\delta \quad (1)$$

The loss factor tan δ (the ratio between G" and G'), and the complex viscosity $|\eta^*|$ (it depends on both G' and G") are displayed in Eq. (2): [52,53]

$$\tan\delta = \frac{G''}{G'}, |\eta^*| = \frac{1}{\omega}\sqrt{G'^2 + G''^2} \quad (2)$$

Table 1 (see below) reports the name and composition of the examined samples. As estimated by repeated measurements, the error in the reported transition temperatures is about ± 0.5 °C.

2.3. SAXS measurements

A S3-MICRO SWAXS camera system (HECUS X-ray Systems, Graz, Austria) equipped with a GeniX x-ray source (50 kV and 1 mA, Cu Ka radiation of 1.542 Å) and a 1D-PSD-50 M system (HECUS X-ray Systems, Graz, Austria) containing 1024 channels of width 54.0 μm was used to carry out small angle X-ray scattering (SAXS) measurements. Quartz capillaries were filled with the F127 sample solutions at 4 °C and then sealed with wax and left at room temperature for 24 h before measurements. All samples were equilibrated for 1 h at the selected temperature, then the SAXS patterns were acquired for 5 h. Measurements were performed at 40 °C using a Peltier device to stabilize and control the temperature.

Errors in the lattice parameters of about 5 % were estimated introducing the q_{ob} values of the most significant peaks in the usual relation $a = (2\pi/q_{ob})d_{hkl}$ where d_{hkl} is the Miller index corresponding to the q_{ob} considered reflection, in agreement with the expected repetition distance of the structure (see Table S1 in Supplementary Material).

2.4. Self-diffusion NMR

A Bruker Ascend™ 600 NMR spectrometer (14.0 T), equipped with an internal temperature control unit was used for ^{1}H NMR experiments (^{1}H frequency 600.13 MHz). ^{1}H NMR self-diffusion coefficients (D) were

Table 1
Compositions, Cmts, T_{hg} and T_{sg} (°C ± 0.5) of F127 formulations. Values obtained from the dynamic heating temperature ramps at ω = 1 Hz and 1 % linear strain.

Sample	Salt conc. (mol/kg)	Cmt (°C)	T_{hg} (°C)	T_{sg} (°C)	Sample	Salt conc. (mol/kg)	Cmt (°C)	T_{hg} (°C)	T_{sg} (°C)
F127 - no salt	0.000	21.2	22.2	69.8	F127 - $MgCl_2$	0.150	17.1	18.1	70.8
F127 - NaCl	0.075	18.1	20.2	71.8	F127 - Na_2SO_4	0.075	17.2	17.3	60.9
F127 - NaCl	0.100	18.1	19.1	70.8	F127 - Na_2SO_4	0.125	15.8	16.2	49.3
F127 - NaCl	0.125	18.1	19.1	71.8	F127 - Na_2SO_4	0.150	13.7	14.8	50.4
F127 - NaCl	0.150	17.1	18.1	69.8	F127 - NaSCN	0.075	20.1	21.2	73.9
F127 - KCl	0.075	18.7	19.8	71.9	F127 - NaSCN	0.125	21.2	21.2	73.9
F127 - KCl	0.125	17.6	18.7	69.8	F127 - NaSCN	0.150	21.2	22.2	73.9
F127 - KCl	0.150	17.6	18.7	69.8					
F127 - $MgCl_2$	0.075	18.1	19.1	71.8	F127 - NaCl	1.000	5.0	6.2	43.1
F127 - $MgCl_2$	0.125	18.1	19.1	67.8	F127 - NaSCN	1.000	27.3	30.3	62.7

determined for H_2O and in some cases for the CH_2 and CH_3 polymer signals (see further below) using the PGSE acquisition sequence (DOSY toolbox). *D* values were calculated by using the Stejskal-Tanner equation,[54–56]

$$I = I_0 e^{-D\gamma^2 g^2 \delta^2 (\Delta - \delta/3)} = I_0 e^{-kD} \quad (3)$$

Where, *I and* I_o are the integral of the peak at each field gradient intensity and the signal intensity in the absence of field gradient, respectively; γ is the magnetogyric ratio, *g*, δ, and Δ are the magnitude, the duration, and the separation of the field gradient pulses, respectively. For polymer self-diffusion experiments: Δ = 999 or 2000 ms and δ = 5 ms were used. Gradient strength in the range 1 – 51 G/cm was used.

The spin echo decays of CH_2 and CH_3 F127 signals were generally non-mono-exponential. Hence, a bi-exponential equation was used:

$$I = I_0 (p_{fast} e^{-kD_{fast}} + p_{slow} e^{-kD_{slow}}) \quad (4)$$

where, D_{fast} and D_{slow} are two diffusion coefficients corresponding to p_{fast} and p_{slow} molar fractions, respectively.[25,57]

The biexponential fitting of Eq. (4) is an approach often used although not rigorous when dealing with polydisperse polymers[58,59] for which the signal decay may be described in terms of a probability density distribution function of diffusion coefficients P(D) as indicated in the following equation [25,58,59]

$$I(k) = I_0 \int_0^\infty P(D) e^{-kD} dD \quad (5)$$

If the functional form of P(D) is unknown, a distribution of the self-diffusion coefficients can however be obtained through the inverse Laplace transformation (ILT) of I(k). Here, the ILT process was carried out using an in-house written Matlab program, according to the work of Whittall and MacKay.[60]

The dimensions of the diffusing species were obtained from a corrected Stokes-Einstein equation which considers the obstruction effects due to the volume fraction of the dispersed phase Φ_P: [61–63]

$$D_P^{obs} = D_P^0 (1 - \kappa \Phi_P) = \frac{k_B T}{6\pi\eta R_P} (1 - \kappa \Phi_P) \quad (6)$$

Where, R_P is the hydrodynamic radius of pluronic F127 at infinite dilution and η is the solvent viscosity. Here, the constant $\kappa = 2.5$ (typical values are 2–4) [63] and a volume fraction of the dispersed phase $\Phi_P \approx 0.1932$ (considering the density of the H_2O/D_2O solvent and of F127 1.006 and 1.05 g/mL [64], respectively) were used for all samples. Viscosity values of the H_2O/D_2O = 80/20 (wt/wt) solvent mixture were obtained using the Arrhenius relation: $\ln \eta_w^\circ = -6.5105 + 1929.1/T$ Pa s, previously reported [18]. Water self-diffusion data in all samples were not considered in the discussion since only a simple dependence on temperature was observed, as demonstrated by the Arrhenius plot reported in Figure S9B (Supplementary Material file).

3. Results and discussion

As described in the experimental section, all samples contained 20 wt % of the polymer Pluronic F127 dissolved in MilliQ water with 20 wt% of D_2O, with a resulting v/v fraction of the dispersed polymer phase $\Phi_P = 0.1932$ in all samples. Salt concentration is referred to the solvent mass (molality) and is given in mol/kg. Salt concentrations from 0.075 to 0.15 mol/kg were considered for NaCl, KCl, $MgCl_2$, Na_2SO_4 and NaSCN. To evaluate the effect of a high concentration of sodium salts on the phase behavior and on the transition temperatures, rheological measurements were also performed using a salt concentration 1 mol/kg for NaCl and NaSCN (concentrations of Na_2SO_4 higher than 0.28 mol/kg induce loss of gelation, thus this salt was not considered[32]). Loss of F127 gelation transition was observed also by adding 1.7–1.8 mol/kg NaCl and other salts at relatively high concentration. [32–34].

3.1. Rheology

Before presenting the results of the present work, we first must note that commercial F127, simply referred as F127, displays a certain variation of composition, and a degree of molecular weight polydispersity;[3,19–25,27,65] this will, however, have only minor effects on the general arguments.[18,25] This is illustrated by differences in the phase behavior of F127, including slightly different transition temperatures for the critical micelle temperature (cmt), the sol–hard gel (T_{hg}) and for the hard gel-soft gel (T_{sg}) transition temperatures. [19,20,23,24,26,27,65] Thermoreversibility for salt-free F127 (20 wt% in water) was ascertained by performing the heating and cooling ramps reported in Supplementary Material Fig. S1A (for storage G' and loss G" modulus) and Fig. S1B (for tan δ).

Fig. 1A displays the dynamic heating temperature ramp obtained for the aqueous solutions of Pluronic F127 (20 wt%) with no added salt. At low temperature there is no self-assembly, and F127 is in the form of unimers, i.e. in a non-associated state: G' < G" (both moduli are relatively low). As temperature increases, polymer solvation decreases, thus the formation of micelles is induced; the critical micelle concentration (CMC) decreases with temperature leading to a concentration dependent "critical micelle temperature" (cmt). Cmt is clearly identified by a maximum in tan δ since G" (the viscous modulus) increases. A further increase of temperature leads to an increase of micelle concentration resulting in a crowding effect and in a crystallization (gelation) of globular micelles into a cubic LC phase (see par 3.2), denoted as "hard gel" (T_{hg}) because of its character. Both G' and G" become very high, with G' > G", and tan δ almost constant. At still higher temperature there is a decreased viscosity resulting from the formation of another cubic phase, denoted as "soft gel" (T_{sg}). The change in rheological properties reflects the fact that with decreased solvation the volume fraction of the micelle decreases, due to the decrease of hydration strength. As the temperature is increased further, solvation is decreased to a point where there is a macroscopic phase separation between F127 and water; this is referred to as "clouding" because of the turbidity of the

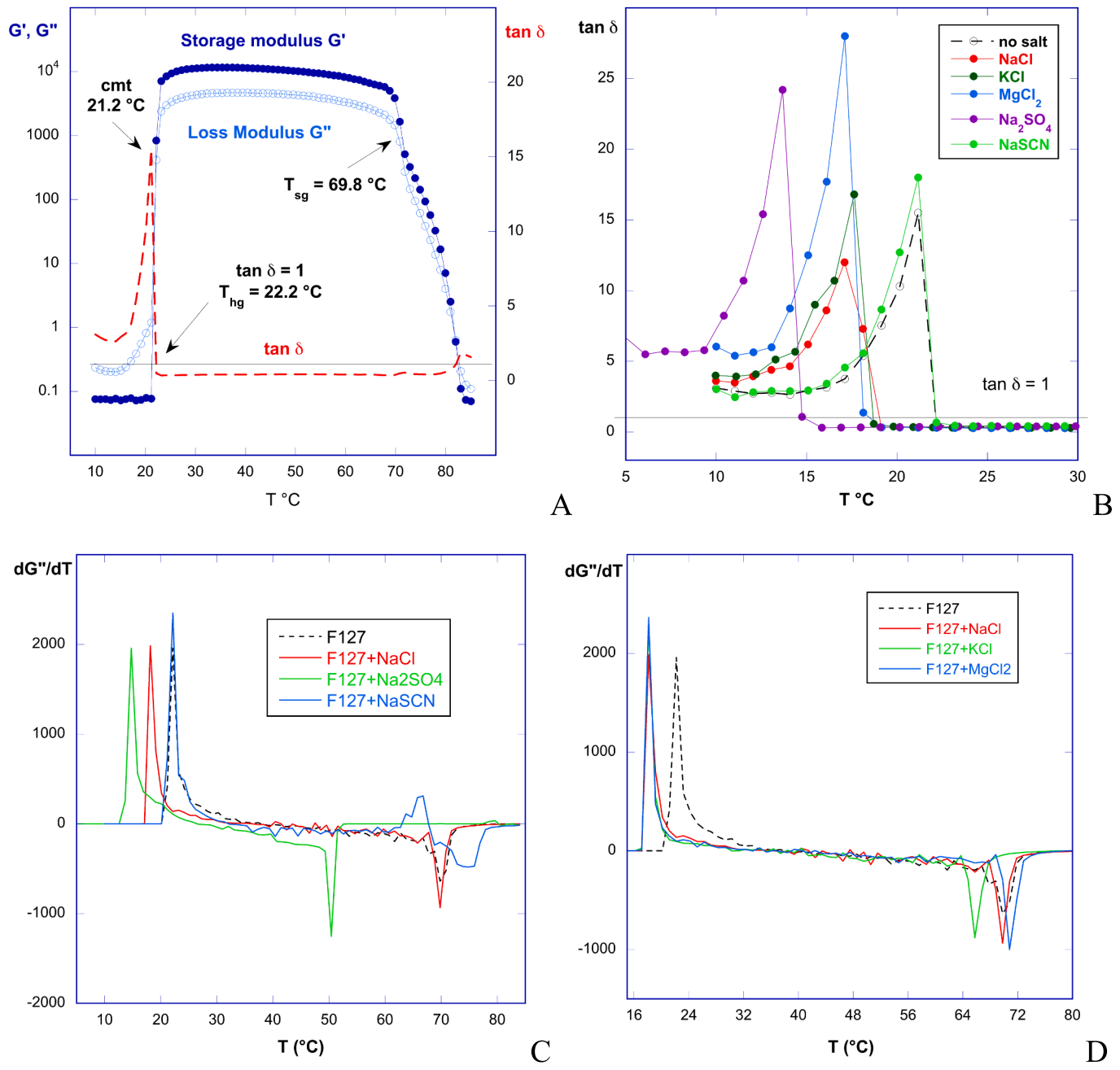

Fig. 1. Rheological data for F127 systems. **(A)** Storage Modulus G' (Pa), Loss Modulus G" (Pa) and tan δ vs. T (10–85 °C) for salt free F127 (20 wt%) sample. **(B-D)** F127 with added salts: Salt-free F127 in black dashed lines. Salt 0.15 mol/kg **B)** tan δ vs. T for all systems, the line corresponding to tan δ = 1 allows to identify T_{hg} values; **C)** dG"/dT (Pa K^{-1}) vs. T for sodium salts; D) dG"/dT (Pa K^{-1}) vs. T for chlorides salts.

system. It can be noted that the other phases, solutions, and cubic phases, are clear.

Fig. 1A shows also the trend of tan δ that allows to clearly identify the cmt from the maximum, and the sol-hard gel transition temperature T_{hg} at tan δ = 1 (G' = G"). The weak maximum of tan δ recorded at high temperature indicates T_{sg}.

Dynamic heating temperature ramps, as in Fig. 1A, were used to investigate the effect of salts on cmts and sol–gel transition temperatures of our F127-based formulations. Data related to heating ramps for F127 systems in the presence of 0.15 mol/kg salts are reported in Supplementary Material Figures S2A for chlorides and Figure S2B for sodium salts. Fig. 1B shows tan δ vs T (10 – 30 °C) for F127 in the absence and in the presence of salts at 0.15 mol/kg. Cmt values are obtained by maximum in tan δ whereas the T_{hg} are the temperatures at which tan δ = 1 occurs for each salt. T_{sg} temperatures are more clearly identified using the trend of dG"/dT vs. T. This is due to the fluctuations of tan δ in the range 35–85 °C as shown in Supplementary Material Figure S2C. Fig. 1C for sodium salts and 1D for chloride salts show dG"/dT vs. T trends where both T_{hg}, and T_{sg} can be identified from the maximum and the minimum, respectively. In the case of NaSCN presented in Fig. 1C we note that dG"/dT trend shows a second small maximum before the minimum associated to T_{sg} (this point will further be discussed below).

Notably, also the storage modulus can be used to describe both gel transition phenomena in F127 systems. However, the hard-soft gel transition is often less marked (a few hundred Pa variation) compared to the sol-hard gel one (several orders of magnitude variation of both moduli), and it is mainly described by viscous dominated dynamics (i.e., much more sensitive to the loss modulus G" contribution). Cmt values

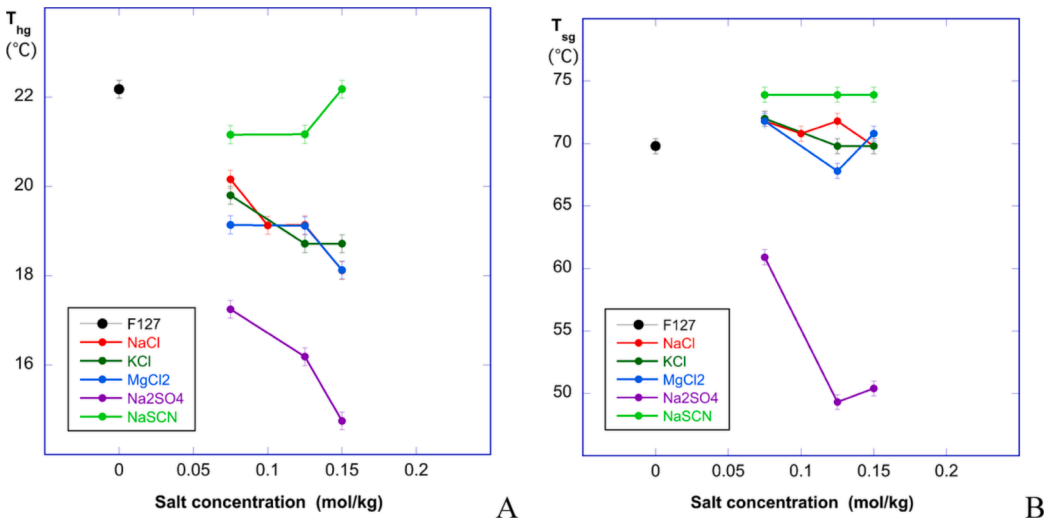

Fig. 2. Transition temperatures for salt-free F127 (black dot) and in the presence of salt (concentration 0.075–0.15 mol/kg). **(A)** Sol – Hard gel temperatures T_{hg}; **(B)** Hard – Soft gel temperatures T_{sg}.

along with T_{hg} and T_{sg} transition temperatures, determined for all examined samples, are reported in Table 1. The effect of the different salts' concentrations on T_{hg} and T_{sg} is shown in Figure 2A and 2B, respectively.

Particularly significant is the decrease of T_{hg} and T_{sg} caused by Na_2SO_4 as highlighted in Figure 2 (see also tan δ values in Fig. 1B and dG"/dT trends in Fig. 1C). We notice that at each concentration (range 0.075–0.15 mol/kg) the sodium salts produce a decrease of cmt in the order $SO_4^{2-} > Cl^- > SCN^- \approx$ no salt. The effect of cations for the chlorides is instead not very significant either on T_{hg} or T_{sg} temperatures as shown in Figure 2. Significant changes of cmt, T_{hg} and T_{sg} temperatures due to 1 mol/kg NaCl or NaSCN addition (see SI Figure S3) were observed as reported in Table 1.

Turning the attention to the effect of NaSCN on F127 rheological behavior, the different dG"/dT vs T trends in the presence of NaSCN at all investigated concentrations are reported in Fig. 3A (F127 non salt and in the presence of 1 mol/kg NaSCN) and 3B (F127 in the presence of 0.075–0.15 mol NaSCN). In the case of 1 mol/kg NaSCN we note an additional minimum at 39.4 °C and additional maximum at 57.7 °C before the minimum associated to T_{sg}.

In the range of T where cubic LC are present, considering that the loss modulus G" represents the viscous contribution, we can reasonably associate a minimum to a swelling of the LC matrix that produces a structural softening as the hard-soft gel transition where stiffness decreases: we can name this transition temperature as T_{2sg}. Conversely, the maximum in the dG"/dT derivative can be related to a crowding effect caused by a temperature increase. In other words, the increase of viscosity, like that observed after the cmt, can be associated to a stiffness increase: we can name this transition temperature as T_{2hg}. These fluctuations in terms of bulk mechanical response suggest significant dispersion interactions between SCN^- anions and the polymer which may involve either the nonpolar PO micellar core or the more polar EO interface, as indicated by the trends reported in Fig. 3. The effect of NaSCN concentration on the temperature dependent structural transitions can be summarized as follows: i) with increasing salt concentration T_{hg} increases (stiffness increases), whereas T_{2hg} decreases; ii) the softening transition defined at T_{2sg} appears only at high salt concentration of NaSCN. These additional transitions can likely be related to the highly

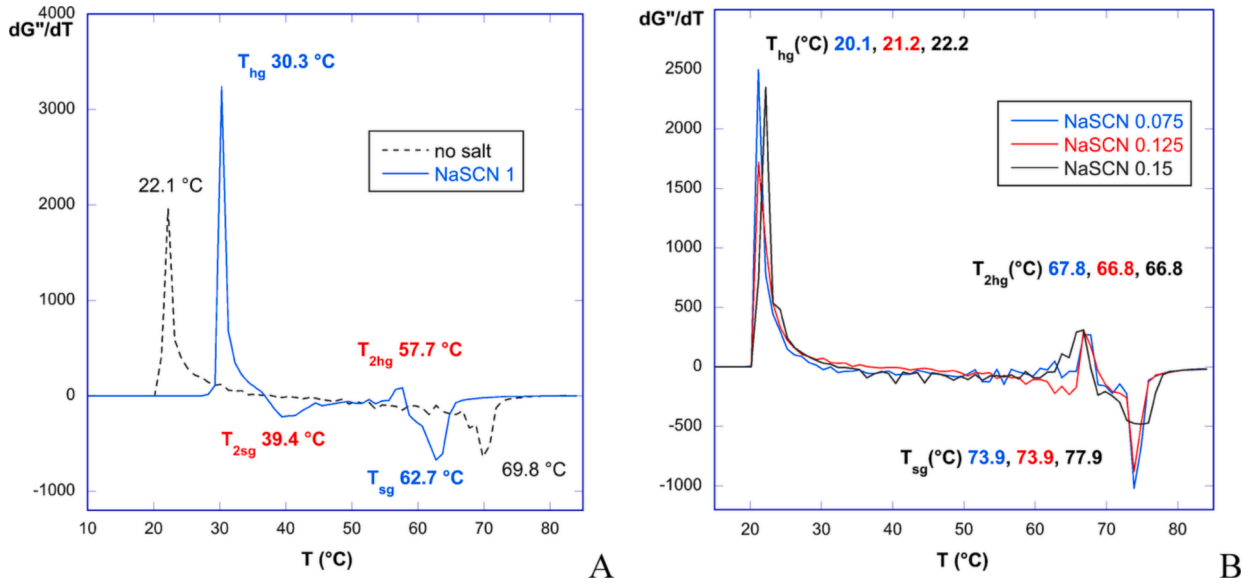

Fig. 3. Phase transitions of F127 in the presence of different concentrations of NaSCN, described by dG"/dT vs. T. A) 1 mol/kg NaSCN compared to salt-free F127; B) NaSCN 0.075–0.15 mol/kg.

chaotropic nature of SCN^- anion whose weak hydration may allow changes in the strength of the interactions with the copolymer groups that in turn undergo the weakening of the hydration upon increasing temperature. Similar fluctuations of rheological behavior were not observed in the presence of the other examined salts even in the case of 1 mol/kg NaCl (see Figure S3 in Supplementary Material).

To summarize the main results, it is worth considering the effect of Na^+ salts at different concentrations on the trend of the modulus of complex viscosity $|\eta^*|$ (Eq. (3) reported in Fig. 4. Indeed, we ascertained that the highest values of both storage and loss modulus as well as of the complex viscosity, are related to the formation of stable hard LC gels. Therefore, $|\eta^*|$, which includes the effect of both storage and loss modulus, allows to clearly identify the range of temperature for which a plateau occurs and where cubic liquid crystals exist and confer stability to the hard gel. Fig. 4 reports the cases of Na_2SO_4 (Fig. 4A), NaCl (Fig. 4B) and NaSCN (Fig. 4C).

The rheological studies provide detailed information on how the self-assembly behavior of F127 is affected by simple electrolytes, including the temperature dependent solvation effects on phase transitions. At lower salt concentrations, the extension of the gel (cubic LC) region is markedly reduced by sulfate, for higher concentrations also by chloride and to lesser extent by thiocyanate. This follows the decreased solvation due to sulfate and an increased one for thiocyanate; chloride is intermediate. The formation of the soft gel (see T_{sg} in Table 1) is highlighted by the sudden drop of complex viscosity that occurs with increasing T.

3.2. Small angle X-ray scattering

Above the sol-hard gel (T_{hg}) transition temperature, the F127 system forms micellar cubic liquid crystals. Depending on the purity of the copolymer, and on the presence of other components, long- range ordered nanostructures having *fcc* (*Fm3m* or *Fd3m*) and *bcc* (*Im3m*), or primitive (*Pm3n* and simple cubic, *SC*) space groups have been recognized.[20–22,26,27,64,66–69] Often cubic structures give rise to only a few intense Bragg peaks. Therefore, indexing is not always unique and straightforward. Here the copolymer volume fraction is relatively low ($\Phi_P = 0.1932$), and SAXS patterns show several weak peaks. Table S1 in Supplementary Material reports details on the repetition distances and Miller indexes for some cubic lattices. The microstructure of some selected samples was investigated through SAXS experiments at 40 °C. All original SAXS patterns and Miller index plots are reported in Supplementary Material. For LC formed by commercial F127 copolymer, *fcc* structures such as *Fm3m* (Q^{225}) have often been reported.[20,27] Our SAXS patterns could also be indexed as Simple Cubic (*SC*) structures.

Fig. 4S (Supplementary Material file) shows the SAXS pattern of F127 without salts where reflections were assigned according to *Fm3m* (Fig. 4SA) and *SC* (Fig. 4SB) lattice structures. However, the good linear relation between the Miller indices d_{hkl} and the observed reflections q_{ob}, displayed in Fig. 4SC and 4SD for *Fm3m* and *SC* lattices, respectively, does not allow to clearly select the most reliable structure. About this, we should recall that a SANS investigation of 19.4 wt% F127 [26] on the basis of the copolymer apolar volume fraction and geometrical considerations, suggested the occurrence of a *SC* structure (lattice parameter in the range 17.0–20.9 nm) at 25 °C. A primitive cubic lattice was also suggested to form at 25 °C adding 5 wt% of butanol to different F127 samples having a copolymer content in the range 25–45 wt%.[64].

The SAXS patterns obtained in the presence of salts of 0.15 mol/kg showed quite diverse intensity of the peaks, particularly those in the ranges $q = 0.02–0.03$ Å^{-1} and $q = 0.05–0.06$ Å^{-1}.[64] Using Miller indices and the observed q_{ob} that can clearly be identified we noted very good linear fittings which, in all cases, closely extrapolate to zero and provide from the slopes more accurate lattice values (Table S2 in Supplementary Material reports either the instrument indexing using the program 3D view, or the Miller index plots along with the obtained lattice parameters). However, as observed in the absence of salts, it is not possible to assign a unique lattice structure to our samples, since in all cases either the *fcc* or the simple cubic structures give a relatively reliable assignment of the main reflections. Very poor SAXS patterns were observed in the presence of Na_2SO_4 (data not reported since sample appeared slightly degraded after 4 h SAXS experiment). This likely occurs because in the presence of this salt all transition temperatures decrease significantly, particularly the hard-soft gel $T_{sg} \approx 50$ °C (see Table 1), hence the stability of the cubic liquid crystals at T = 40 °C, used in the SAXS experiment, may be affected. Table 2 summarizes SAXS data obtained using the q_{ob} (Å^{-1}) values that could clearly be assigned according to Miller indices for the *Fm3m* and *SC* lattice cells.

The interfacial area per EO block A_P, and the micellar aggregation number N_{ag} are other features that can be obtained from the SAXS analysis, as previously reported;[66–69] these data are also reported in Table 2. Briefly, assuming that PO blocks are highly segregated in the micellar hydrophobic core and considering that PO blocks constitute 33.2 % of the copolymer volume whose volume fraction in all samples is $\Phi_P = 0.1932$, the total apolar volume φ is approximately given by the relation $\varphi = 0.332\Phi_P = 0.064$.[66–70].

The φ value equals the volume fraction of the N_m micelles (average spherical radius R of the hydrophobic core) in the cubic unit cell having lattice parameter a

$$\varphi = \frac{N_m}{a^3}\left(\frac{4\pi R^3}{3}\right) \quad (7)$$

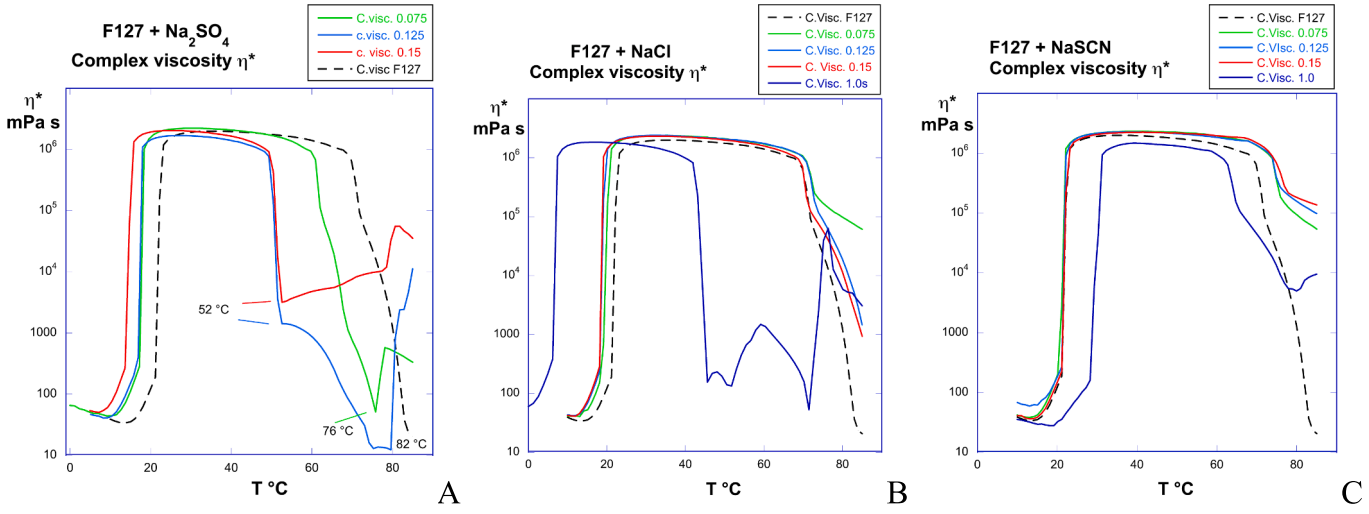

Fig. 4. The modulus of complex viscosity $|\eta^*|$ vs. T for different salt concentrations: **A**) Na_2SO_4; **B**) NaCl; **C**) NaSCN.

Table 2
SAXS data at 40 °C. F127 20 wt% in water (H_2O/D_2O = 80/20) without salts and with salts 0.15 mol/kg. SAXS lattice parameters a (Å) for Fm3m and Simple cubic (SC) structures, obtained from Miller plots (see Table S1 in SI). The interfacial area A_P (eq. (8)) per EO block, and the aggregation number N_{ag} (eq. (9)) of F127 micelles are also reported.

Sample	*a (Å)* *Fm3m* Miller	A_P(Å^2) *Fm3m*	N_{ag} *Fm3m*	*a (Å)* *SC* Miller	A_P(Å^2) *SC*	N_{ag} *SC*
F127 No salt	301.2	211.4	66	178.1	225.2	55
F127 + NaCl	317.9	200.2	78	220.3	182.1	103
F127 + KCl	358.9	177.4	112	183.4	218.7	60
F127 + $MgCl_2$	332.8	191.3	89	207.9	192.9	87
F127 + NaSCN	395.9	160.8	150	220.4	182.0	103

Considering that the molecular volume of F127 is $V_P \approx 20 \times 10^3$ Å^3 [68] the interfacial area per EO block A_P can be calculated according to the following relation:

$$A_P = (36\pi N_m \varphi^2)^{1/3} \frac{V_P}{2\Phi_P a} \quad (8)$$

The micellar aggregation number N_{ag} is calculated according to the following relation:

$$N_{ag} = \frac{\Phi_P a^3}{N_m V_P} \quad (9)$$

In Eq. (8) the number of micelles $N_m = 4$ and $N_m = 1$ were used for *Fm3m* and *SC* lattice structures, respectively. Salt addition induces a clear increase of the lattice parameter (*a)* and consequently a decrease of the interfacial area A_P per EO group, along with an increase of the aggregation number N_{ag} in agreement with Eqs. (7) and (8). Likely due to the large amount of water and the relatively low concentration of the added salts, we cannot identify significant specific ion effects on the cubic LC structures at 40 °C. We can just observe that the most chaotropic anion SCN^-, because of a strong interaction with both EO and PO groups of the copolymer, mainly due to its high polarizability, induces the largest increase of the lattice parameter and favors the growing of micelles: this can particularly be seen in SAXS data indexed as *Fm3m* structure. Notably, interfacial area values around 200 Å^2 and aggregation numbers around 50–80 (or higher in the presence of salts) have previously been reported.[16,26,71] In our calculations we may notice that the use of *SC* assignment gives equal lattice parameters, and hence equal A_P and N_{ag} values in the presence of NaCl and NaSCN: this is not consistent with the expected specific ion effects. However, if the relatively low intensity of SAXS peaks and the approximations introduced in Eqs. 7–9 are considered, the above observation cannot safely be used to choose the *Fm3m* (*fcc* structure) lattice as the best data modeling. The whole of SAXS data, despite the difficulties related to the identification of the most reliable cubic lattice, clearly proves the occurrence of stable cubic LC in the presence of added salts, at temperatures around 40 °C; this implies that the formulation applied at body temperatures may offer a significant resistance towards dilution effects induced by the contact with body fluids.

3.3. Self-diffusion NMR

Selected samples were analyzed by means of the NMR self-diffusion technique. A sample of F127 without added salt, having $\Phi_P = 0.193$, was investigated at 6 different temperatures in the range from 16 to 55 °C. NMR self-diffusion spin-echo decays were obtained for the $-CH_2$ (signal at ≈ 3.6 ppm) and $-CH_3$ (signal at ≈ 1.1 ppm) (Figure S9A in SI). The echo-decays observed for the CH_2 NMR signals at different temperatures, given in semilogarithmic plots (according to Eq. (3), are shown in Figure 5A. Echo-decays at temperatures higher than 16 °C are clearly not mono-exponential, while the decay at 16 °C can reasonably well be modeled by a single exponential form (Eq. (3); see fit in Figure 5A: r = 0.997). Therefore, at temperatures above 16 °C, a bi-exponential fitting of the NMR echo-decay (Eq. (4) [18,25] was used to obtain the self-diffusion coefficients, D_{fast} and D_{slow}, that can be related to the populations, in terms of the molar fraction p_{fast} and p_{slow}, of free unimers and micellar aggregates, respectively (we are neglecting any effects caused by different NMR relaxation times in the two populations)[25,57–59,65]. It should be noted that the lowest T = 16 °C is below the cmt, thus no significant aggregation should be expected. This behavior is clearly depicted by the ILT analysis of the echo decay of the CH_2 and CH_3 signals reported in Figure S9B and S9C where the occurrence of more than a single population, for T ≥ 16 °C, is highlighted. Figure 5B shows the trend of D_{fast}, D_{slow} and p_{fast} calculated by means of a bi-exponential fitting of CH_2 and CH_3 NMR signal according to Eq. (4) (see data reported in Table S3 in SI). Self-diffusion coefficients (mono-exponential fitting) at 16 °C for both CH_2 and CH_3 signals are included in the plots as single symbols indicated as D_{16}.

NMR data obtained for F127 without salts at different temperatures suggest the following main features: i) after the sol–gel transition the deviation from mono-exponentiality reflects the polydispersity in the F127 sample.[25,58,59] The ILT plots in Figure S9B-S9C give a clear picture of the observed behavior of salt-free F127; ii) the p_{fast} values are significantly lower for the CH_3 signal (see p_{fast} in Figure 5B), indicating that the more PO-rich (containing the CH_3 fragment) part in the distribution of the F127 molecules are aggregated to a larger extent; in other words, there are more hydrophobic species in the aggregates; iii) the diffusion coefficients of the free F127, D_{fast}, increase with increasing T (more for the CH_2-fragment), reflecting also the decreased water viscosity.

The F127 present as unimers diffuses “freely”, with values determined by obstruction effects from the micellar aggregates and trivial viscosity effects from the water solvent. The diffusion process of the aggregated F127 corresponds to a random walk among the stationary aggregates and its rate is determined by the life-time of F127 in the aggregates, which in turn is given by the concentration of each species in the water solvent, and the distance between the aggregates.

In the presence of 0.15 mol/kg salt, NMR self-diffusion data were collected at 16 °C, below the cmt, and at 40 °C, after the main sol - gel transition T_{hg} for all systems.

Fig. 6 shows echo-decays with and without salts at 16 °C and 40 °C. At 16 °C (Fig. 6A) the effects of the addition of salts results in changes in the appearance of the echo decays with the magnitude of changes in the following order: (no salt) < NaSCN < KCl ≈ $MgCl_2$ ≤ NaCl < Na_2SO_4, which corresponds to a Hofmeister series (Table S4 in SI). [42,72].

At 40 °C there are only minimal effects due to the salts as reported in Fig. 6B. The trends are more clearly highlighted by the inverse Laplace transformation (ILT) of the CH_2 echo-decay shown in Fig. 6C (16 °C) and 6D (40 °C).

The salts used, except for NaSCN where the influence is the smallest, can be characterized as “salting-out” salts, the effects of which are to decrease the solubility (and cloud point) of the polymer and hence to induce aggregate formation.[25] The onset of aggregation leads to a more curved echo-decay in the representation of Fig. 6A and 6B. We note that the same trend is observed in the rheological data, particularly in the complex viscosity data (see SI Table S5). The complex viscosity values at 16 °C are relatively low, around 40–140 mPa s (except the case of Na_2SO_4 sample, see SI, Table S5) and increase in the following order: (no salt) < NaSCN < NaCl ≈ KCl < $MgCl_2$ ≪ Na_2SO_4, namely the Hofmeister series again. At 40 °C, when all systems form cubic LC, complex viscosity values are very high, around 10^3 Pa s, and increase in the order Na_2SO_4 < (no salt) < NaCl ≈ KCl < $MgCl_2$ ≈ NaSCN. At 40 °C the salt addition appears to have little effect on the aggregation process in the sense that the distribution among unimers and aggregated F127

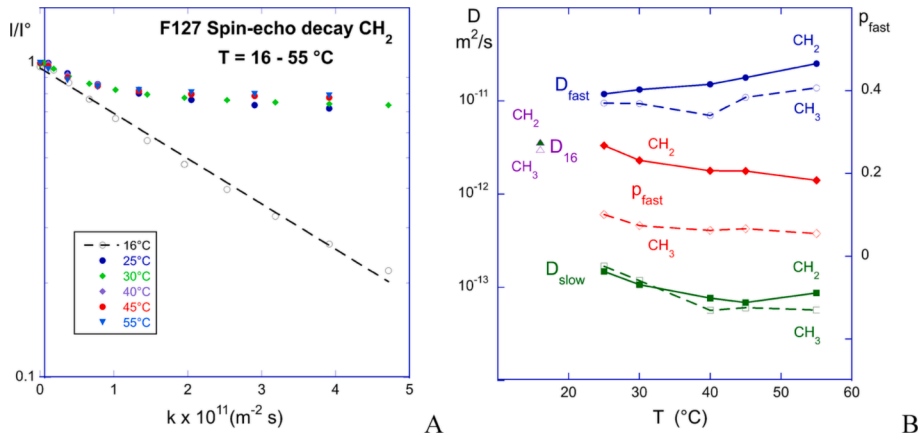

Fig. 5. NMR self-diffusion data for salt-free F127 sample at different temperatures (see data in Table S3). (A) NMR self-diffusion data for F127 sample without salts at different temperatures. PGSE echo decays of the CH_2 signal, I/I° vs k, according to Eq. (3) (semilog plot): the straight line for the decay at 16 °C is included merely for reference. (B) D_{fast}, D_{slow} and p_{fast} from bi-exponential fittings of CH_2 (filled symbols and continuous lines) and CH_3 (empty symbols and dashed lines) NMR signals at 25, 30, 40, 45 and 55 °C according to Eq. (4). At 16 °C the D_{16} values (monoexponential fitting using Eq.3) for both CH_2 (filled symbol) and CH_3 (empty symbol) signals are included in the plot as single violet symbols. (For interpretation of the references to colour in this figure legend, the reader is referred to the web version of this article.)

molecules is not affected, giving no measurable effects on the echo decays.

Thus, at 40 °C, the NMR echo-decays can reasonably well be modeled by a bi-exponential fitting with small variations in both D values and in the intensity distribution of the fast and slow components as highlighted by the ILT plot in Fig. 6D. These findings are of great interest in view of the potential applications of the formulations in diverse biomedical contexts. This may further be confirmed by calculating the dimensions of the free diffusing species. The radius was calculated through Eq. (6) only for the D_{fast} values of CH_2 NMR signals introducing $\kappa\Phi_P = 0.5$ to account for obstruction effect. R values in the range 9–12 nm were calculated for F127 unimers without added salts, at the different temperatures (see Table S6 in Supplementary Material). In the presence of salts R values in the range 10–13 nm at 16 °C, and in the range 7–10 nm at 40 °C (see Table S7 in Supplementary Material) were calculated. These data confirm that in the range of T = 30–40 °C, the micellar cubic LCs are thermodynamically stable also in the presence of relatively low concentration (0.15 mol/kg) of different salts.

3.4. Considerations on the F127/salt-based thermosensitive platform

To provide novel smart drug delivery performance F127/salt thermosensitive formulations should display some important features as highlighted in many previous works.[11–15,28,31,33] Besides the biocompatibility request, the most important features are related not only to all transition temperatures but also to the stiffness and to the resistance of the hard gel phase towards dilution due to the contact with biological fluids. For instance, the stiffness of the formulation can allow for a more sustainable release.[16].

Table 3 summarizes the most important data obtained through rheological measurements. Focusing on the chlorides that are classified as fully biocompatible, we may note that T_{hg} values around or lower than 20 °C (see also Table 1) prevent intramuscular or intravenous injections administration route. However, it may be of interest that the range of stability of the 'hard gel' is not significantly dependent on the salt, whereas the highest values of the complex viscosity and the storage modulus (elastic component) are observed at lower T and increase with respect to F127 alone.

In addition, focusing on the temperature at which the highest value of complex viscosity $|\eta^*|$ occurs for sodium salts, we note that these temperatures agree with the Hofmeister series for the anions. Thus SCN^- gives the highest temperatures of the different transitions and of the viscosity maximum whereas SO_4^{2-} gives the lowest ones.

Notably, chlorides are certainly a suitable and biocompatible choice for F127 based formulations to be used for external applications. NaCl is commonly used as added salt in drug delivery systems because of its high biocompatibility, but the present data suggest that also $MgCl_2$ can be considered as a suitable alternative that, if needed, may provide a higher ionic strength due the divalent cation. The use of KCl instead is not generally considered a suitable choice because of the associated hyperkalemia risk factors. These results are furthermore corroborated by observing that SAXS analysis provides similar results for NaCl and $MgCl_2$, in terms of lattice parameters (around 300 and 200 Å for *Fm3m* and *SC* structures respectively), apolar interfacial area ($A_P \approx$ 180–200 $Å^2$), and aggregation numbers ($N_{ag} \approx$ 80–100). NMR data, particularly the distribution of the self-diffusion coefficients at 40 °C reported in Fig. 6B, clearly demonstrate that replacing NaCl with $MgCl_2$, although the increase of ionic strength from 0.15 to 0.45 due to the presence of the divalent cation, does not influence intermolecular interactions above the sol–gel temperatures. Indeed, molecular motions of free F127 molecules within the medium made of micellar cubic LC gels do not change significantly in the presence of the different salts as shown by the ILT plot in Fig. 6C.

4. Concluding remarks

The increasing interest of thermoresponsive Pluronic-based formulations for widespread applications in nanomedicine, [11,12,15,16,18,28,59,71] is mainly due to the fact that these copolymers are involved in clinical trials,[51] and this motivated us to study the effect on the phase behavior of salts added at physiological concentrations (around 0.15 mol/kg). The use of rheology along with SAXS measurements and NMR self-diffusion allowed to highlight the following new features related to the performance of a F127/salt-based formulations. In comparison with previous rheological works [23,24,53] on F127 polymer, this study presents how the use of simple heating ramps can provide detailed information on cmt and transition temperatures that can clearly be identified by the trends of tan δ and dG"/dT as a function of T. In summary, SAXS and NMR data, together with the observed high complex viscosity, indicate that F127-based formulations, in the presence of physiological amounts of biocompatible salts such as NaCl or $MgCl_2$, give a tunable thermosensitive drug delivery platform, characterized by high stiffness and suitable transition temperatures. Particularly the high stiffness may assure a sustained drug release and provide a prolonged resistance to dilution due to contact with body fluids, in the wide range of temperature, 30–45 °C, where

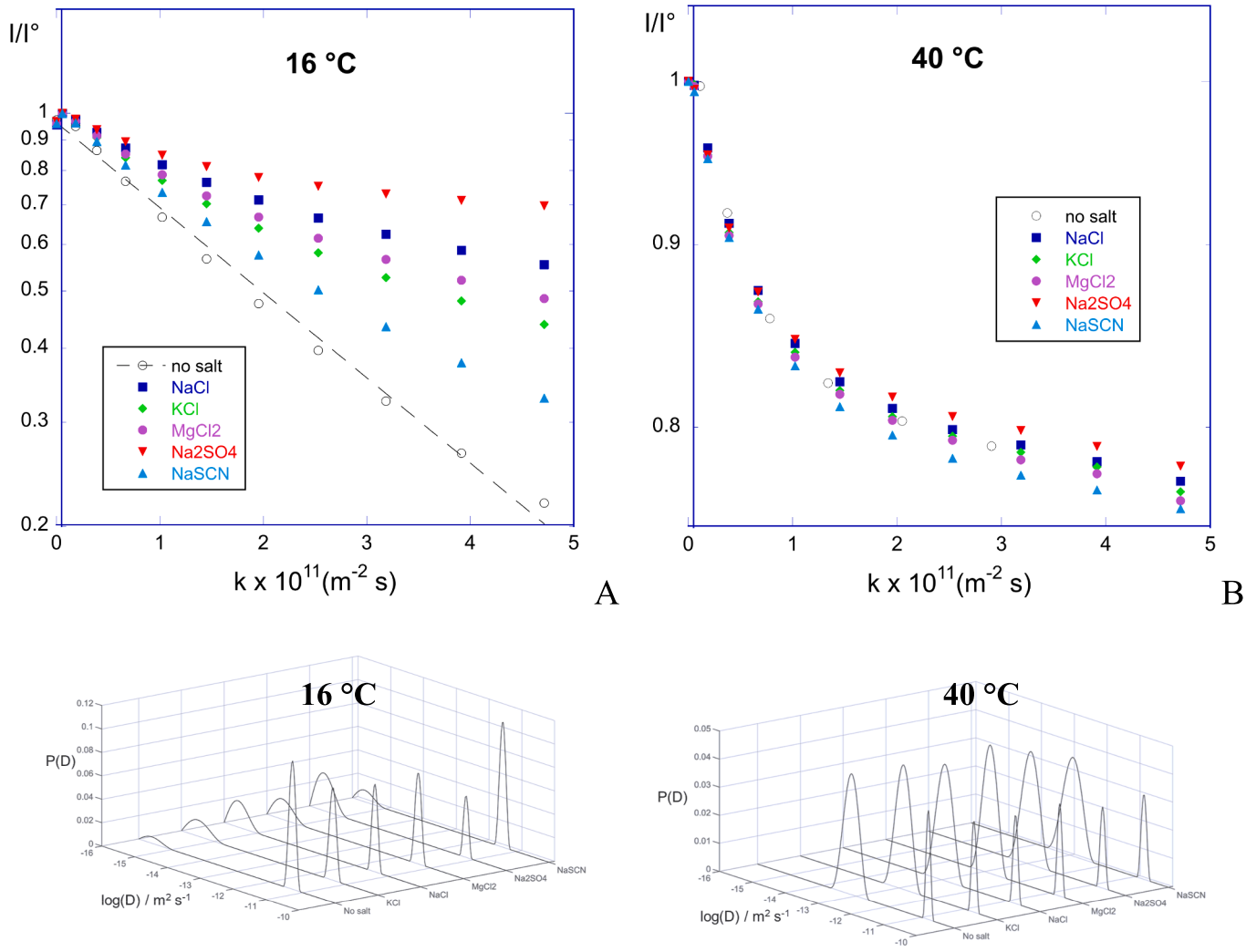

Fig. 6. Echo-decays of the CH_2 NMR signal at 3.5 ppm with and without salts at 16 °C (A) and 40 °C (B). I/I° vs k according to Eq. (3), salt concentration 0.15 mol/kg. The corresponding distribution of the diffusion coefficients D from ILT analysis. Log D vs. P(D) where P(D) is the value of the distribution function of D at that value of D, in a.u. ILT plots of the NMR echo-decay at 16 °C (C) and 40 °C (D).

Table 3
Cmt and T_{hg} - T_{sg} transition temperatures for F127 without salts and with 0.15 mol/kg salt. Column 4 reports the T at which the maximum complex viscosity η* (column 5) is observed, along with the G' and G" values (columns 6 and 7) measured at the same T (max η*).

Sample salt 0.15 mol/kg	Cmt °C	T_{hg} - T_{sg} °C	T (max η*) °C	η* 10^6 Pa s	G' 10^4 Pa	G" 10^3 Pa
F127 no salt	21	22–70	35.0	1.99	1.16	4.64
F127-NaCl	17	18–70	32.0	2.32	1.40	4.18
F127-KCl	18	19—70	34.0	2.31	1.40	4.00
F127-$MgCl_2$	17	18—71	33.0	2.34	1.42	3.88
F127-Na_2SO_4	14	15–50	24.5	2.04	1.20	4.57
F127-NaSCN	21	22–74	41.0	2.25	1.34	4.46

cubic liquid crystals are thermodynamically stable. Future work is needed to test these formulations in the presence of drugs and using simulated body fluids, involving the simultaneous presence of different salts and buffers.

CRediT authorship contribution statement

Giovanni Russo: Conceptualization, Formal analysis, Investigation, Methodology. **G. Rossella Delpiano:** Investigation. **Cristina Carucci:** Investigation. **Massimiliano Grosso:** Conceptualization, Investigation, Writing – original draft. **Claudia Dessì:** Investigation. **Olle Söderman:** Conceptualization, Investigation, Methodology, Supervision, Writing – original draft, Writing – review & editing. **Björn Lindman:** Conceptualization, Methodology, Supervision, Writing – original draft. **Maura Monduzzi:** Conceptualization, Funding acquisition, Methodology, Project administration, Supervision, Writing – original draft, Writing – review & editing. **Andrea Salis:** Conceptualization, Data curation, Formal analysis, Funding acquisition, Methodology, Project administration, Supervision, Validation, Writing – original draft, Writing – review & editing.

Declaration of competing interest

The authors declare that they have no known competing financial interests or personal relationships that could have appeared to influence the work reported in this paper.

Data availability

Data will be made available on request.

Acknowledgements

C.C. thanks CSGI and Fondazione di Sardegna (F72F20000230007) for funding her post doc. Thanks are due to CeSAR (Centro Servizi di Ateneo per la Ricerca) of the University of Cagliari for the use of NMR facilities, and particularly to Dr. Sandrina Lampis for her essential technical support. O.S. thanks the Division of Physical Chemistry, Lund University, for financial support. B.L. acknowledges the Coimbra Chemistry Centre (CQC) FCT through the Project UID/QUI/00313/2020.

Appendix A. Supplementary data

Supplementary data to this article can be found online at https://doi.org/10.1016/j.eurpolymj.2023.112714.

References

[1] B. Kronberg, K. Holmberg, B. Lindman, Surface Chemistry of Surfactants and Polymers, John Wiley & Sons, Ltd, Chichester, UK, 2014. https://doi.org/10.1002/9781118695968.
[2] M. Malmsten, Biopolymers at Interfaces, CRC Press (2003), https://doi.org/10.1201/9780824747343.
[3] M. Malmsten, B. Lindman, Self-assembly in aqueous block copolymer solutions, Macromolecules. 25 (1992) 5440–5445, https://doi.org/10.1021/ma00046a049.
[4] M. Malmsten, B. Lindman, Effects of homopolymers on the gel formation in aqueous block copolymer solutions, Macromolecules. 26 (1993) 1282–1286, https://doi.org/10.1021/ma00058a014.
[5] P. Alexandridis, Poly(ethylene oxide)/poly(propylene oxide) block copolymer surfactants, Curr Opin Colloid, Interface Sci. 2 (1997) 478–489, https://doi.org/10.1016/S1359-0294(97)80095-7.
[6] P. Alexandridis, B. Lindman, Amphiphilic Block Copolymers, Elsevier (2000), https://doi.org/10.1016/B978-0-444-82441-7.X5000-2.
[7] A. Gandhi, A. Paul, S.O. Sen, K.K. Sen, Studies on thermoresponsive polymers: Phase behaviour, drug delivery and biomedical applications, Asian, J Pharm Sci. 10 (2015) 99–107, https://doi.org/10.1016/j.ajps.2014.08.010.
[8] F.D. Jochum, P. Theato, Temperature- and light-responsive smart polymer materials, Chem Soc Rev. 42 (2013) 7468–7483, https://doi.org/10.1039/c2cs35191a.
[9] D. Schmaljohann, Thermo- and pH-responsive polymers in drug delivery, Adv Drug Deliv Rev. 58 (2006) 1655–1670, https://doi.org/10.1016/j.addr.2006.09.020.
[10] P.D. Thornton, R.J. Mart, R.V. Ulijn, Enzyme-responsive polymer hydrogel particles for controlled release, Advanced Materials. 19 (2007) 1252–1256, https://doi.org/10.1002/adma.200601784.
[11] E. Alvarado-Gomez, G. Martínez-Castañon, R. Sanchez-Sanchez, A. Ganem-Rondero, M.J. Yacaman, F. Martinez-Gutierrez, Evaluation of anti-biofilm and cytotoxic effect of a gel formulation with Pluronic F-127 and silver nanoparticles as a potential treatment for skin wounds, Materials Science and Engineering: c. 92 (2018) 621–630, https://doi.org/10.1016/j.msec.2018.07.023.
[12] E. Kushan, E. Senses, Thermoresponsive and Injectable Composite Hydrogels of Cellulose Nanocrystals and Pluronic F127, ACS Appl Bio Mater. 4 (2021) 3507–3517, https://doi.org/10.1021/acsabm.1c00046.
[13] N. Zeng, G. Dumortier, M. Maury, N. Mignet, V. Boudy, Influence of additives on a thermosensitive hydrogel for buccal delivery of salbutamol: Relation between micellization, gelation, mechanic and release properties, Int J Pharm. 467 (2014) 70–83, https://doi.org/10.1016/j.ijpharm.2014.03.055.
[14] E. Jin, Z. Zhang, H. Lian, X. Chen, C. Xiao, X. Zhuang, X. Chen, Injectable electroactive hydrogels based on Pluronic® F127 and tetraaniline copolymer, Eur Polym J. 88 (2017) 67–74, https://doi.org/10.1016/j.eurpolymj.2017.01.013.
[15] Y.J. Kim, Y.T. Matsunaga, Thermo-responsive polymers and their application as smart biomaterials, J Mater Chem b. 5 (2017) 4307–4321, https://doi.org/10.1039/c7tb00157f.
[16] P. Hiwale, S. Lampis, G. Conti, C. Caddeo, S. Murgia, A.M. Fadda, M. Monduzzi, In Vitro Release of Lysozyme from Gelatin Microspheres: Effect of Cross-linking Agents and Thermoreversible Gel as Suspending Medium, Biomacromolecules. 12 (2011) 3186–3193, https://doi.org/10.1021/bm200679w.
[17] A. Fakhari, J. Anand Subramony, Engineered in-situ depot-forming hydrogels for intratumoral drug delivery, Journal of Controlled Release. 220 (2015) 465–475, https://doi.org/10.1016/j.jconrel.2015.11.014.
[18] M. Monduzzi, G. Musu, M. Grosso, C. Carucci, B. Lindman, O. Söderman, A. Salis, Effect of electrolytes on the sol–gel phase transitions in a Pluronic F127/carboxymethyl cellulose aqueous system: Phase map, rheology and NMR self-diffusion study, Eur Polym J. 181 (2022), 111707, https://doi.org/10.1016/j.eurpolymj.2022.111707.
[19] G. Wanka, H. Hoffmann, W. Ulbricht, Phase Diagrams and Aggregation Behavior of Poly(oxyethylene)-Poly(oxypropylene)-Poly(oxyethylene) Triblock Copolymers in Aqueous Solutions, Macromolecules. 27 (1994) 4145–4159, https://doi.org/10.1021/ma00093a016.
[20] K. Mortensen, Y. Talmon, Cryo-TEM and SANS Microstructural Study of Pluronic Polymer Solutions, Macromolecules. 28 (1995) 8829–8834, https://doi.org/10.1021/ma00130a016.
[21] K. Mortensen, Structural studies of aqueous solutions of PEO - PPO - PEO triblock copolymers, their micellar aggregates and mesophases; a small-angle neutron scattering study, Journal of Physics: Condensed Matter. 8 (1996) A103–A124, https://doi.org/10.1088/0953-8984/8/25A/008.
[22] K. Mortensen, Structural properties of self-assembled polymeric micelles, Curr Opin Colloid, Interface Sci. 3 (1998) 12–19, https://doi.org/10.1016/S1359-0294(98)80036-8.
[23] S. Liu, L. Li, Multiple Phase Transition and Scaling Law for Poly(ethylene oxide)–Poly(propylene oxide)–Poly(ethylene oxide) Triblock Copolymer in Aqueous Solution, ACS Appl Mater Interfaces. 7 (2015) 2688–2697, https://doi.org/10.1021/am507749w.
[24] C. Chaibundit, N.M.P.S.P.S. Ricardo, F. de M.L.L. Costa, S.G. Yeates, C. Booth, Micellization and Gelation of Mixed Copolymers P123 and F127 in Aqueous Solution, Langmuir. 23 (2007) 9229–9236. https://doi.org/10.1021/la701157j.
[25] M. Nilsson, B. Håkansson, O. Söderman, D. Topgaard, Influence of Polydispersity on the Micellization of Triblock Copolymers Investigated by Pulsed Field Gradient Nuclear Magnetic Resonance, Macromolecules. 40 (2007) 8250–8258, https://doi.org/10.1021/ma071302p.
[26] R.K. Prud'homme, G. Wu, D.K. Schneider, Structure and Rheology Studies of Poly(oxyethylene−oxypropylene−oxyethylene) Aqueous Solution, Langmuir. 12 (1996) 4651–4659, https://doi.org/10.1021/la951506b.
[27] K. Mortensen, W. Batsberg, S. Hvidt, Effects of PEO−PPO Diblock Impurities on the Cubic Structure of Aqueous PEO−PPO−PEO Pluronics Micelles: fcc and bcc Ordered Structures in F127, Macromolecules. 41 (2008) 1720–1727, https://doi.org/10.1021/ma702269c.
[28] S. Chatterjee, P.C. Hui, C. Kan, W. Wang, Dual-responsive (pH/temperature) Pluronic F-127 hydrogel drug delivery system for textile-based transdermal therapy, Sci Rep. 9 (2019) 11658, https://doi.org/10.1038/s41598-019-48254-6.
[29] Q. Zhang, C. Weber, U.S. Schubert, R. Hoogenboom, Thermoresponsive polymers with lower critical solution temperature: from fundamental aspects and measuring techniques to recommended turbidimetry conditions, Mater Horiz. 4 (2017) 109–116, https://doi.org/10.1039/C7MH00016B.
[30] G.-E. Yu, Y. Deng, S. Dalton, Q.-G. Wang, D. Attwood, C. Price, C. Booth, Micellisation and gelation of triblock copoly(oxyethylene/oxypropylene/oxyethylene), F127, Journal of the Chemical Society, Faraday Transactions. 88 (1992) 2537, https://doi.org/10.1039/ft9928802537.
[31] G. Dumortier, J.L. Grossiord, F. Agnely, J.C. Chaumeil, A Review of Poloxamer 407 Pharmaceutical and Pharmacological Characteristics, Pharm Res. 23 (2006) 2709–2728, https://doi.org/10.1007/s11095-006-9104-4.
[32] N. Pandit, Loss of gelation ability of Pluronic® F127 in the presence of some salts, Int J Pharm. 145 (1996) 129–136, https://doi.org/10.1016/S0378-5173(96)04748-5.
[33] M. Bohorquez, C. Koch, T. Trygstad, N. Pandit, A Study of the Temperature-Dependent Micellization of Pluronic F127, J Colloid Interface Sci. 216 (1999) 34–40, https://doi.org/10.1006/jcis.1999.6273.
[34] N. Pandit, T. Trygstad, S. Croy, M. Bohorquez, C. Koch, Effect of salts on the micellization, clouding, and solubilization behavior of pluronic F127 solutions, J Colloid Interface Sci. 222 (2000) 213–220, https://doi.org/10.1006/jcis.1999.6628.
[35] F. Hofmeister, Zur Lehre von der Wirkung der Salze, Archiv Für Experimentelle Pathologie Und Pharmakologie. 24 (1888) 247–260, https://doi.org/10.1007/BF01918191.
[36] W. Kunz, J. Henle, B.W. Ninham, "Zur Lehre von der Wirkung der Salze" (about the science of the effect of salts): Franz Hofmeister's historical papers, Curr Opin Colloid, Interface Sci. 9 (2004) 19–37, https://doi.org/10.1016/j.cocis.2004.05.005.
[37] B. Kang, H. Tang, Z. Zhao, S. Song, Hofmeister Series: Insights of Ion Specificity from Amphiphilic Assembly and Interface Property, ACS Omega. 5 (2020) 6229–6239, https://doi.org/10.1021/acsomega.0c00237.
[38] Y. Marcus, Surface Tension of Aqueous Electrolytes and Ions, J Chem Eng Data. 55 (2010) 3641–3644, https://doi.org/10.1021/je1002175.
[39] Y. Marcus, Individual ionic surface tension increments in aqueous solutions, Langmuir. 29 (2013) 2881–2888, https://doi.org/10.1021/la3041659.
[40] Y. Marcus, Specific ion effects on the surface tension and surface potential of aqueous electrolytes, Curr Opin Colloid, Interface Sci. 23 (2016) 94–99, https://doi.org/10.1016/j.cocis.2016.06.016.
[41] Y. Marcus, A relationship between the effect of uni-univalent electrolytes on the structure of water and on its volatility, Journal of Chemical Physics. 148 (2018), https://doi.org/10.1063/1.5009311.
[42] A. Salis, B.W. Ninham, Models and mechanisms of Hofmeister effects in electrolyte solutions, and colloid and protein systems revisited, Chem Soc Rev. 43 (2014) 7358–7377, https://doi.org/10.1039/c4cs00144c.
[43] D.F. Parsons, C. Carucci, A. Salis, Buffer-specific effects arise from ionic dispersion forces, Physical Chemistry Chemical Physics. 24 (2022) 6544–6551, https://doi.org/10.1039/D2CP00223J.
[44] Y. Zhang, P. Cremer, Interactions between macromolecules and ions: the Hofmeister series, Curr Opin Chem Biol. 10 (2006) 658–663, https://doi.org/10.1016/j.cbpa.2006.09.020.

[45] R. Breslow, T. Guo, Surface tension measurements show that chaotropic salting-in denaturants are not just water-structure breakers, Proceedings of the National Academy of Sciences. 87 (1990) 167–169, https://doi.org/10.1073/pnas.87.1.167.
[46] B. Lindman, G. Karlström, Nonionic polymers and surfactants: Temperature anomalies revisited, Comptes Rendus Chimie. 12 (2009) 121–128, https://doi.org/10.1016/j.crci.2008.06.017.
[47] E. Thormann, On understanding of the Hofmeister effect: how addition of salt alters the stability of temperature responsive polymers in aqueous solutions, RSC Adv. 2 (2012) 8297, https://doi.org/10.1039/c2ra20164j.
[48] Y. Zhang, S. Furyk, D.E. Bergbreiter, P.S. Cremer, Specific ion effects on the water solubility of macromolecules: PNIPAM and the Hofmeister series, J Am Chem Soc. 127 (2005) 14505–14510, https://doi.org/10.1021/ja0546424.
[49] M. Boström, D.F. Parsons, A. Salis, B.W. Ninham, M. Monduzzi, Possible Origin of the Inverse and Direct Hofmeister Series for Lysozyme at Low and High Salt Concentrations, Langmuir. 27 (2011) 9504–9511, https://doi.org/10.1021/la202023r.
[50] A. Salis, F. Cugia, D.F. Parsons, B.W. Ninham, M. Monduzzi, Hofmeister series reversal for lysozyme by change in pH and salt concentration: insights from electrophoretic mobility measurements, Physical Chemistry Chemical Physics. 14 (2012) 4343, https://doi.org/10.1039/c2cp40150a.
[51] A.P. Constantinou, T.K. Georgiou, Pre-clinical and clinical applications of thermoreversible hydrogels in biomedical engineering: a review, Polym Int. 70 (2021) 1433–1448, https://doi.org/10.1002/pi.6266.
[52] C.W. Macosko, Rheology Principles, Measurements and Applications, Wiley-vch, New York, 1994.
[53] K. Suman, S. Sourav, Y.M. Joshi, Rheological signatures of gel–glass transition and a revised phase diagram of an aqueous triblock copolymer solution of Pluronic F127, Physics of Fluids. 33 (2021), 073610, https://doi.org/10.1063/5.0057090.
[54] P. Stilbs, Fourier transform pulsed-gradient spin-echo studies of molecular diffusion, Prog Nucl Magn Reson, Spectrosc. 19 (1987) 1–45, https://doi.org/10.1016/0079-6565(87)80007-9.
[55] P. Stilbs, K. Paulsen, Global least-squares analysis of large, correlated spectral data sets and application to chemical kinetics and time-resolved fluorescence, Review of Scientific Instruments. 67 (1996) 4380–4386, https://doi.org/10.1063/1.1147539.
[56] W.S. Price, Pulsed-field gradient nuclear magnetic resonance as a tool for studying translational diffusion: Part II, Experimental Aspects, Concepts Magn Reson. 10 (1998) 197–237, https://doi.org/10.1002/(SICI)1099-0534(1998)10:4<197::AID-CMR1>3.0.CO;2-S.
[57] J. Jansson, K. Schillén, M. Nilsson, O. Söderman, G. Fritz, A. Bergmann, O. Glatter, Small-angle X-ray scattering, light scattering, and NMR study of PEO-PPO-PEO triblock copolymer/cationic surfactant complexes in aqueous solution, Journal of Physical Chemistry b. 109 (2005) 7073–7083, https://doi.org/10.1021/jp0468354.
[58] M. Nydén, O. Söderman, An NMR Self-Diffusion Investigation of Aggregation Phenomena in Solutions of Ethyl(hydroxyethyl)cellulose, Macromolecules. 31 (1998) 4990–5002, https://doi.org/10.1021/ma971472+.
[59] G. D'Errico, L. Paduano, A. Khan, Temperature and concentration effects on supramolecular aggregation and phase behavior for poly(propylene oxide)-b-poly(ethylene oxide)- b-poly(propylene oxide) copolymers of different composition in aqueous mixtures, 1, J Colloid Interface Sci. 279 (2004) 379–390, https://doi.org/10.1016/j.jcis.2004.06.063.
[60] K.P. Whittall, A.L. MacKay, Quantitative interpretation of NMR relaxation data, Journal of Magnetic Resonance 84 (1989) (1969) 134–152, https://doi.org/10.1016/0022-2364(89)90011-5.
[61] G.M. Bell, Self-diffusion of ions in the electric fields of spherical particles, Transactions of the Faraday Society. 60 (1964) 1752, https://doi.org/10.1039/tf9646001752.
[62] B. Faucompré, B. Lindman, Self-association of zwitterionic and nonionic surfactants, NMR Self-Diffusion Studies, Journal of Physical Chemistry. 91 (1987) 383–389, https://doi.org/10.1021/j100286a027.
[63] K. Zhang, M. Jonstroemer, B. Lindman, Interaction between Nonionic Micelles and a Nonionic Polymer Studied by Fourier Transform NMR Self-Diffusion, J Phys Chem. 98 (1994) 2459–2463, https://doi.org/10.1021/j100060a038.
[64] P. Holmqvist, P. Alexandridis, B. Lindman, Phase Behavior and Structure of Ternary Amphiphilic Block Copolymer−Alkanol−Water Systems: Comparison of Poly(ethylene oxide)/Poly(propylene oxide) to Poly(ethylene oxide)/Poly(tetrahydrofuran) Copolymers, Langmuir. 13 (1997) 2471–2479, https://doi.org/10.1021/la960819j.
[65] M. Shaikhullina, A. Khaliullina, R. Gimatdinov, A. Butakov, V. Chernov, A. Filippov, NMR relaxation and self-diffusion in aqueous micellar gels of pluronic F-127, J Mol Liq. 306 (2020), 112898, https://doi.org/10.1016/j.molliq.2020.112898.
[66] P. Alexandridis, U. Olsson, B. Lindman, Self-Assembly of Amphiphilic Block Copolymers: The (EO)13(PO)30(EO)13-Water-p-Xylene System, Macromolecules. 28 (1995) 7700–7710.
[67] P. Alexandridis, U. Olsson, B. Lindman, Structural Polymorphism of Amphiphilic Copolymers: Six Lyotropic Liquid Crystalline and Two Solution Phases in a Poly(oxybutylene)- b -poly(oxyethylene)−Water−Xylene System, Langmuir. 13 (1997) 23–34, https://doi.org/10.1021/la960733q.
[68] P. Holmqvist, P. Alexandridis, B. Lindman, Modification of the Microstructure in Poloxamer Block Copolymer−Water−"Oil" Systems by Varying the "Oil" Type, Macromolecules. 30 (1997) 6788–6797, https://doi.org/10.1021/ma970625q.
[69] P. Holmqvist, P. Alexandridis, B. Lindman, Modification of the microstructure in block copolymer-water-"oil" systems by varying the copolymer composition and the "oil" type: Small-angle X-ray scattering and deuterium-NMR investigation, J. Phys. Chem. b. 102 (1998) 1149–1158. http://www.scopus.com/inward/record.url?eid=2-s2.0-0031997487&partnerID=40&md5=284703b3d9d329c8be3436d12dcff280.
[70] P. Alexandridis, U. Olsson, B. Lindman, Phase behavior of amphiphilic block copolymers in water-oil mixtures: The pluronic 25R4-water-p-xylene system, J. Phys. Chem. 100 (1996) 280–288. http://www.scopus.com/inward/record.url?eid=2-s2.0-33749430113&partnerID=40&md5=20648bb7ca22c5c62aaf984a7329d7fc.
[71] P.R. Desai, N.J. Jain, R.K. Sharma, P. Bahadur, Effect of additives on the micellization of PEO/PPO/PEO block copolymer F127 in aqueous solution, Colloids Surf A Physicochem Eng Asp. 178 (2001) 57–69, https://doi.org/10.1016/S0927-7757(00)00493-3.
[72] D.F. Parsons, A. Salis, Hofmeister effects at low salt concentration due to surface charge transfer, Curr Opin Colloid, Interface Sci. 23 (2016) 41–49, https://doi.org/10.1016/j.cocis.2016.05.005.